Journal of Sound and Vibration (1976) **47**(2), 147–161

TRANSMISSION OF LOW-FREQUENCY INTERNAL SOUND THROUGH PIPE WALLS

G. F. KUHN† AND C. L. MORFEY

Institute of Sound and Vibration Research,
University of Southampton, Southampton SO9 5NH, England

(*Received* 6 *November* 1975)

Transmission loss measurements are reported for long steel pipes of circular cross-section, with air inside and out, excited by internal sound. At low frequencies (wavelength greater than the pipe diameter), most of the radiated sound is accounted for by pipe bending waves. In order to approach the much higher transmission loss predicted for pure breathing motion of the pipe, bending waves must be suppressed; this has been achieved for a straight pipe by careful isolation. A sharp 90° bend in the pipe is shown to cause significant bending-wave excitation when plane waves are incident on the bend.

1. INTRODUCTION

The transmission through circular pipe walls of internally propagating sound has been studied theoretically by Cremer [1] and Heckl [2]. Both authors developed statistical models of the transmission process, in which the sound field inside the pipe was represented by a random collection of wavefronts or duct modes. In addition, Heckl carried out measurements of sound transmission which agreed fairly well with results from his statistical model in the frequency range for which it was valid ($k_o r_i > 3$, i.e., multi-mode acoustic propagation; a list of symbols is given in Appendix I). At lower frequencies, Heckl's experiments pointed to asymmetry in the acoustic excitation as an important factor in determining how much sound escapes through the walls of the pipe.

The low-frequency measurements in reference [2], together with further data obtained by Small [3], were shown by Morfey [4] to be incompatible with a purely axisymmetric breathing-mode response of the pipe to internal sound waves. Specifically, in the range $k_o r_i < 1{\cdot}8$ where only plane waves propagate along the pipe and a breathing-mode model might be expected to apply, the transmitted sound power as measured by Heckl and Small was up to 30 dB higher than would be estimated from such a model.

All the measurements mentioned above were made on steel cylinders in air, for which a large transmission loss is predicted because of the high stiffness of the axisymmetric breathing mode. However, Brown and Rennison [5] have recently reported reasonable agreement with the breathing-mode prediction using a thin-walled pipe ($h/a = 0{\cdot}03$) of rigid PVC. The combination of small h/a and low Young's modulus‡ in their experiments brought the breathing-mode transmission loss down into the range measured by Heckl and Small for steel pipes.

Further experiments on steel pipes in air in the plane-wave region are described below. Results are presented which show that the increased sound transmission in this region, relative to the idealized axisymmetric model, is due to radiation from pipe bending waves. A major cause of bending-wave excitation is shown to be locally non-uniform sound pressure distributions such as occur in the vicinity of a source, or at bends in the pipe. Above the (1,0) mode cut-off frequency ($k_o r_i = 1{\cdot}841$) bending-wave excitation extends along the whole length

† Now at Department of Commerce, National Bureau of Standards, Washington, D.C. 20234, U.S.A.
‡ E for rigid PVC is around 1/70 of the value for steel.

of the pipe; below the (1,0) cut-off, bending-wave excitation by (1,0) mode acoustic pressures is still possible, but the excitation is localized and can be decoupled from the remainder of the pipe as demonstrated below. Holograms are also shown to illustrate the non-axisymmetric response of a pipe to the acoustic near field of a source.

Finally, the introduction of a 90° bend in an otherwise straight pipe run is shown to cause significant extra sound radiation, as a result of pipe bending waves excited by plane sound waves incident on the bend. The effect is more pronounced with mitred rather than radiused bends.

2. EXPERIMENTAL PROCEDURE

The experiments were performed in a set of one anechoic and two reverberant rooms, as shown in Figure 1. The pipe was acoustically driven with third-octave bands of random noise from the anechoic room end. For the preliminary experiments the arrangement of Figure 1 was used, with a single loudspeaker bolted directly to a flange at the end of the pipe. In subsequent tests two loudspeakers were used, mounted on a separate section of pipe which was decoupled mechanically from the test section, as shown in Figure 2.

The piping runs from the anechoic room, through a hole in the intervening door, into the first reverberant room (see Figure 1). The pipe crosses the reverberant room in an uninterrupted span of 14 ft 4 in (4·37 m) and leaves through a hole in the doors separating the two reverberant rooms. Once in the large reverberant room, the steel pipe is terminated by a plastic hose which leads out of the room. The test section, whose acoustic radiation is to be measured, is the length of pipe within reverberant room No. 1.

To minimize flanking transmission of sound between rooms, the holes in the doors were sealed with lead flanges (4 lb/ft^2), with foam rubber, and with plasticine in the smaller cracks. The resulting noise reduction measured between the adjacent reverberant rooms was 54 dB in the 2 and 2·5 kHz third-octave bands, and higher in the remainder of the test range (315 Hz to 8 kHz). Comparable noise reductions were measured between the anechoic room and reverberant room No. 1.

Since the sound pressure levels in all three rooms during testing were similar, it can be concluded that flanking transmission from either of the adjacent rooms into the test room (reverberant room No. 1) makes a negligible contribution to the level in the test room. The sound power measured in reverberant room No. 1 may therefore be attributed entirely to radiation from the pipe test section.

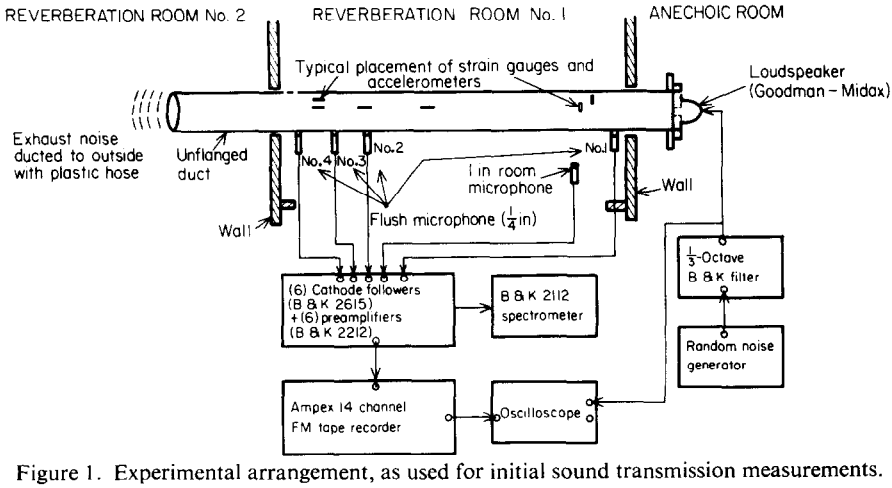

Figure 1. Experimental arrangement, as used for initial sound transmission measurements.

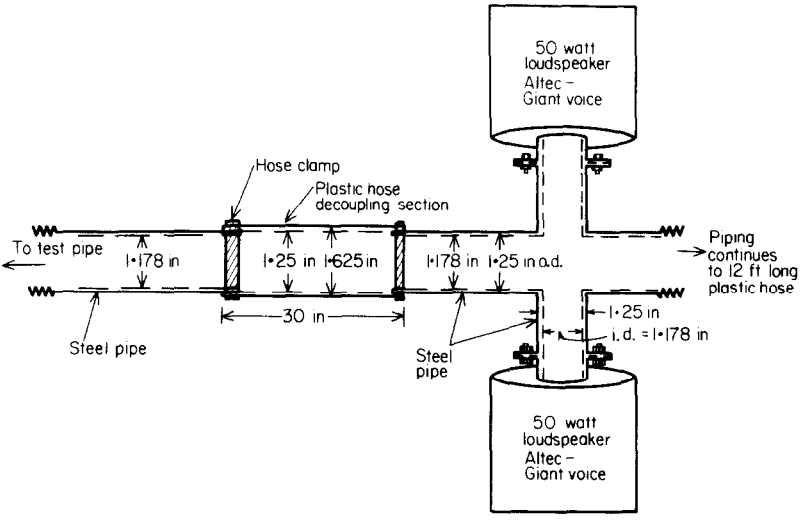

Figure 2. Acoustic source arrangement used for subsequent measurements.

The acoustic pressure inside the pipe was initially measured with four Brüel & Kjaer $\frac{1}{4}$ inch flush-mounted microphones, as shown in Figure 3. In later experiments only two microphones were used, those designated No. 1 and No. 2 in Figure 1. Each of the $\frac{1}{4}$ inch microphones (Type 4135) is seated in a cavity (Figure 3), which couples to the pipe and has a Helmholtz resonance around 21 kHz so as to give a flat pressure response in the frequency range of interest. The average of the mean square pressures measured by the different microphones is used to estimate the total sound power in the pipe (sum of forward and backward wave contributions) in any given third-octave band. Thus if $\langle p^2 \rangle$ is the mean square pressure averaged with respect to position†, the internal power flow assuming only plane waves in the pipe is estimated as

$$W_{\text{int}} = \langle p^2 \rangle S/\rho_0 c_0. \tag{1}$$

The sound power radiated by the pipe wall over the test section is obtained from third-octave sound pressure level measurements taken in reverberant room No. 1 with a Brüel & Kjaer 1 inch microphone. The bandwidth is sufficient to generate a diffuse sound field in the room.

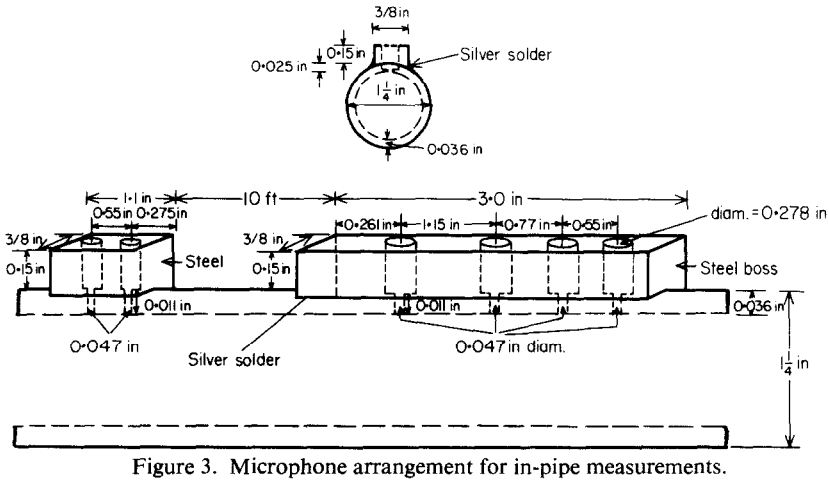

Figure 3. Microphone arrangement for in-pipe measurements.

† Standing-wave effects were less than 0·5 dB, as a result of attenuation in the plastic hose at the end of the test section and the finite frequency bandwidth.

Based on the measured values of radiated sound power (W_{rad}) and total in-pipe power flow (W_{int}), a transmission loss† for the test section is calculated as

$$\mathrm{TL} = 10 \log_{10} W_{int}/W_{rad} \ (\mathrm{dB}). \tag{2}$$

Also of interest is the radiation efficiency of the test section, given by

$$\sigma = W_{rad}/\rho_o c_o S_{rad} \langle u^2 \rangle. \tag{3}$$

The mean square value of the surface normal velocity, u, was measured in third-octave bands by five 2 gram accelerometers, placed arbitrarily along and around the pipe; the results were then averaged to provide an estimate of the mean square velocity over the radiating surface.

A block diagram of the electronic measurement apparatus is given in Figure 1.

3. RESULTS

The results are presented in three sections, covering (1) preliminary transmission loss measurements, (2) an investigation of the means by which pipe bending modes were being excited, and (3) further detailed measurements of transmission loss including the effect of pipe bends.

3.1. INITIAL TL MEASUREMENTS

Preliminary measurements were made with two pipes of the same outer diameter but different wall thicknesses. The sound source in this case was a Goodman–Midax 25 watt loudspeaker bolted directly to the end of the pipe as in Figure 1. The results are shown in Figure 4, where the transmission loss of each pipe is plotted against frequency.

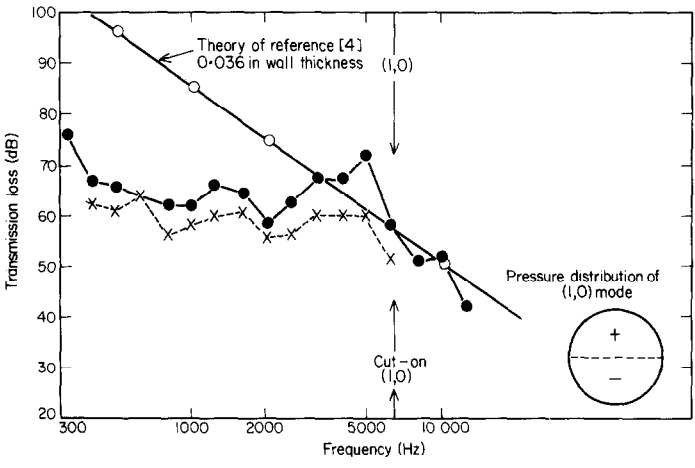

Figure 4. Comparison of third-octave transmission loss measurements on steel pipes of different wall thicknesses; ●——●, 0·036 in; ×----×, 0·092 in. Pipe outer diameter is 1·25 in in both cases. Breathing-mode prediction for the thin-walled pipe is shown as a solid line, ——.

Also shown in Figure 4 is the transmission loss predicted for the thin-walled pipe, assuming the pipe response to be a purely axisymmetric breathing motion driven by plane waves in the pipe. This assumption gives [4]‡

$$W_{rad}/W_{int} \simeq (S_{rad}/2h^2)(\rho_o^2 c_o/\rho_s^2 c_L)(\omega a/c_L)^3. \tag{4}$$

† The transmission loss defined by equation (2) depends on the test length; note that the definition differs from that of Heckl [2] which was used in reference [4].

‡ A factor ½ omitted from equation (7) of reference [4] has been included.

The discrepancy at low frequencies is evident and amounts to about 30 dB; in this respect the results resemble those of Heckl [2] and Small [3] mentioned earlier. Low-frequency discrepancies of the same order have also been reported by Gel'fgat *et al.* [6]. Furthermore, the transmission loss measured for the thick-walled pipe is less than that of the thin-walled pipe, in contradiction to equation (4).

In view of the care taken to eliminate it, flanking transmission into the test room was ruled out as an explanation for the low TL measurements, and attention was turned to pipe bending waves as a source of extra sound radiation. Excitation of bending waves may result either from non-uniform acoustic pressures on the inside of the pipe, or from mechanical vibration of the loudspeaker housing and mounting; experiments were designed to determine which mechanism was operating in the present tests.

3.2. INVESTIGATION OF BENDING-WAVE EXCITATION MECHANISM

3.2.1. *Mechanical isolation tests*

Figure 5 shows the experimental arrangement for investigating the bending-wave excitation mechanism. Mass can be added to the flanges to reduce the mechanical transmission of bending waves into the test pipe. Further mechanical decoupling can be provided by means of a rubber insert between the loudspeaker and the pipe flange. The effect of these modifications on the level of vibration in the test pipe is shown in Figure 6; the measurements were taken

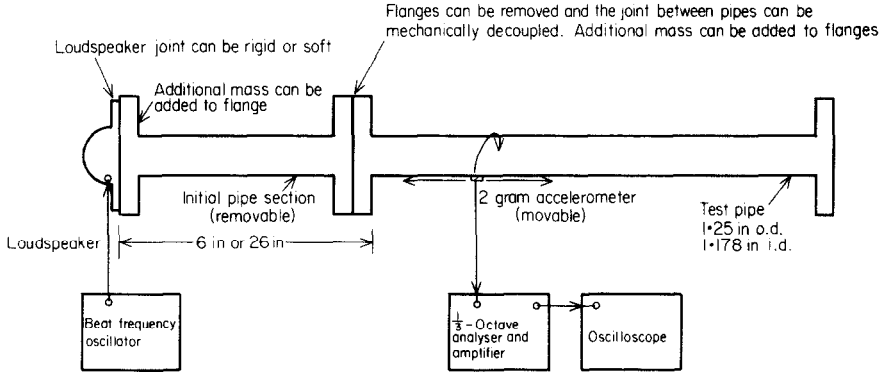

Figure 5. Vibration test of pipe driven by loudspeaker, with varying degrees of mechanical isolation.

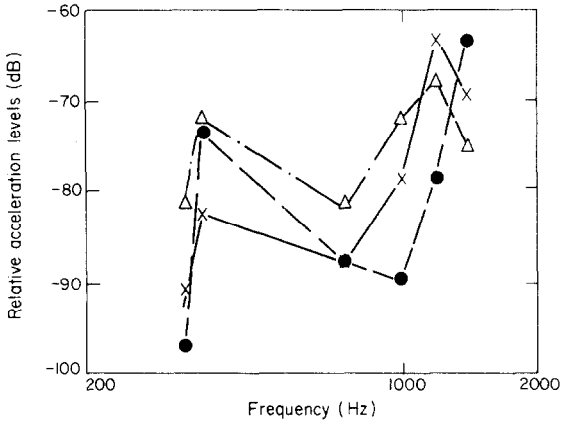

Figure 6. Effect of loudspeaker mounting on maximum acceleration level of test pipe, with 26 in initial section bolted to test pipe. ●——●, Loudspeaker bolted to pipe flange; ×——×, flange mass increased 50%; △—·—△, ½ in foam rubber insert.

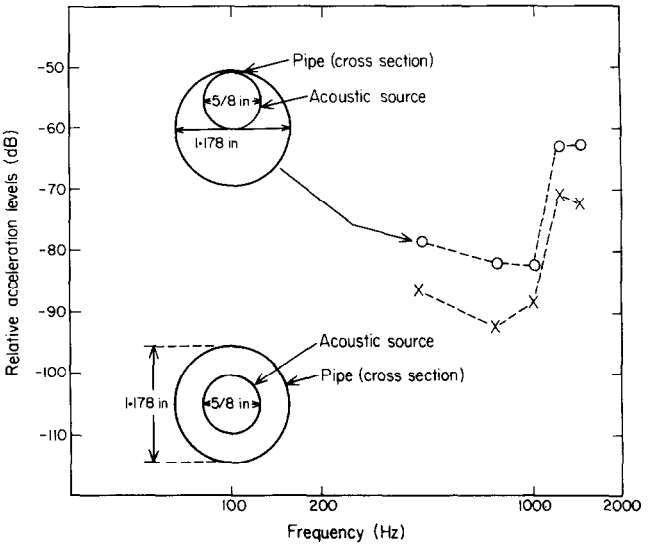

Figure 7. Effect of placing loudspeaker off-axis on maximum acceleration level of test pipe, with initial section removed. ×,○ refer to on-, off-axis source location.

with a hand-held 2 gram accelerometer, and the maximum acceleration level along the pipe (referred to 1 volt on the spectrometer) was recorded at each driving frequency for each of the configurations.

No consistent change in vibration level was produced by either of the mechanical isolation techniques. This suggests that the pipe vibration is due principally to the acoustic near field of the loudspeaker. If the excitation is acoustic, moving the loudspeaker off-axis should increase the pipe vibration, since the (1,0) acoustic mode will be driven more strongly; this was tried, and the results shown in Figure 7 support the acoustic excitation hypothesis.

In order to test the hypothesis further, mechanical isolation was introduced some distance along the pipe rather than at the loudspeaker. This was achieved by mounting the loudspeaker axisymmetrically (as judged by eye) on a separate section of pipe, either 6 in or 26 in long,

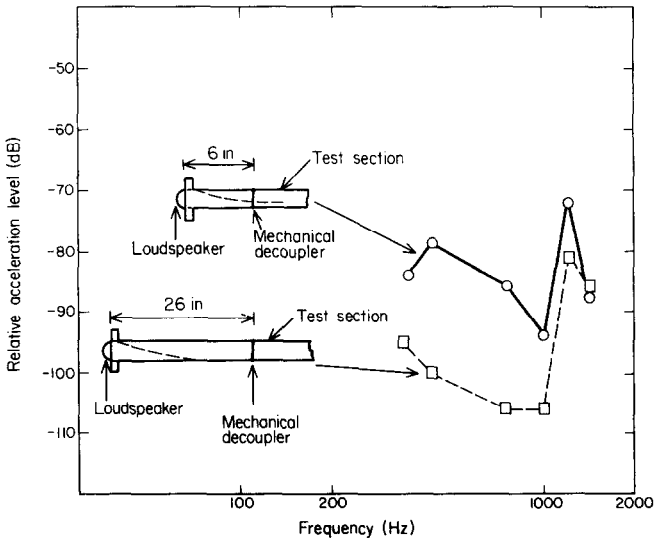

Figure 8. Effect of mechanical isolation from loudspeaker on maximum acceleration level of test pipe. ○——○, 6 in initial section; □——□, 26 in initial section.

which was connected with plasticine to the test pipe—see Figure 8. The 26 in pipe should allow the loudspeaker near field to decay completely within the decoupled section, as indicated by the dashed line in the sketch. The vibration measurements in Figure 8 show that the remote-decoupling arrangement gave a 10–20 dB reduction in pipe vibration at low frequencies, when compared with the other configurations tested.

The conclusion drawn from these tests is that acoustic excitation of pipe bending waves is responsible for the low TL values obtained initially (section 3.1), and that it can be eliminated only by mechanically decoupling the test section *sufficiently far from the source* that the (1,0) acoustic mode has decayed to a negligible amplitude.

3.2.2. *Holographic visualization of pipe motion*

The non-axisymmetric nature of the pipe response can be clearly seen in Figures 9 and 10, which are photographs of holograms. The fringes represent contours of equal amplitude vibration and they thereby delineate the structural mode(s) excited in the pipe. The pipe in this case is the 26 inch section, cantilevered at the source end and driven by a 50 watt Altec Giant Voice. The free end was plugged to minimize the sound escaping into the laboratory.

Figure 9 shows that at 770 Hz the first clamped-free bending mode is excited, presumably by the (1,0) acoustic mode in the source near field. The calculated natural frequency for the bending mode is 70 Hz.

Figure 10 shows the pipe response at 3483 Hz. The $n = 2$ distortional mode of the pipe can be detected; the lowest natural frequency for modes of this circumferential order is 2600 Hz.

Although this pipe is shorter and the end conditions are different from those of the test section, the internal acoustic pressure excitation is the same as for the test section. The holograms show that even under conditions of nominally axisymmetric excitation, the response of a cylindrical pipe is far from axisymmetric.

3.3. FURTHER TL MEASUREMENTS

3.3.1. *Plastic hose coupling to source*

In the light of the results described above, further transmission loss measurements were planned, with the source arrangement shown in Figure 2. The loudspeaker section was joined to the test pipe by a 30-inch length of flexible plastic hose, to minimize the excitation of bending waves in the test pipe.

The measurements of section 3.1 were repeated, first with a straight pipe and then with various 90° bends added to the pipe beyond the straight test section. Figure 11 shows the general arrangement of the source, piping and transducers for these tests.

The transmission loss (TL) values obtained for the straight pipe are shown in Figure 12, together with the axisymmetric-response TL prediction [4]. The discrepancy noted in earlier results is greatly reduced, and between 1 and 5 kHz the measurements lie within −5 to +1 dB of the predicted line. The measured TL below 1 kHz still falls appreciably short of the axisymmetric prediction, although decoupling the acoustic source has produced an increase of some 2–8 dB relative to the earlier measurements.

Introducing a 90° bend in the pipe beyond the test section generally reduces the low-frequency transmission loss. The effect is particularly pronounced (7–14 dB) for the mitred bend in the frequency range 400–1250 Hz, as Figure 12 shows. At higher frequencies the various bent-pipe values lie either side of the straight-pipe TL curve, with no consistent trend apparent between them.

Finally, the transmission loss for both straight and bent pipes drops by around 20 dB between 5 and 6·3 kHz, corresponding to the transition between cut-off and cut-on of the

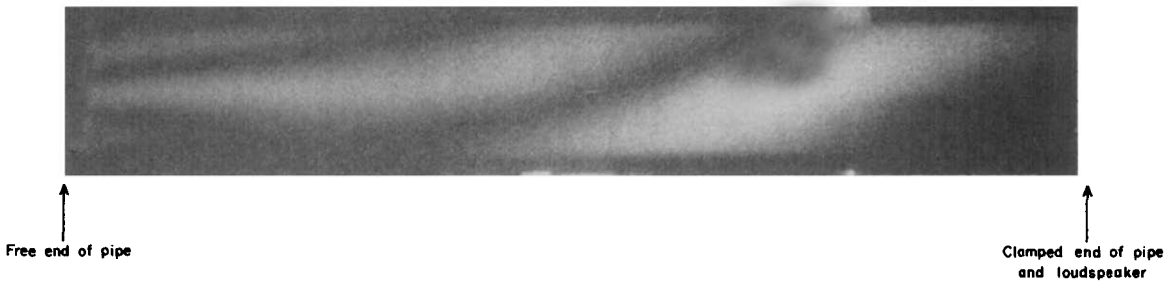

Figure 9. Holographic visualization of acoustically-excited pipe vibration at 770 Hz.

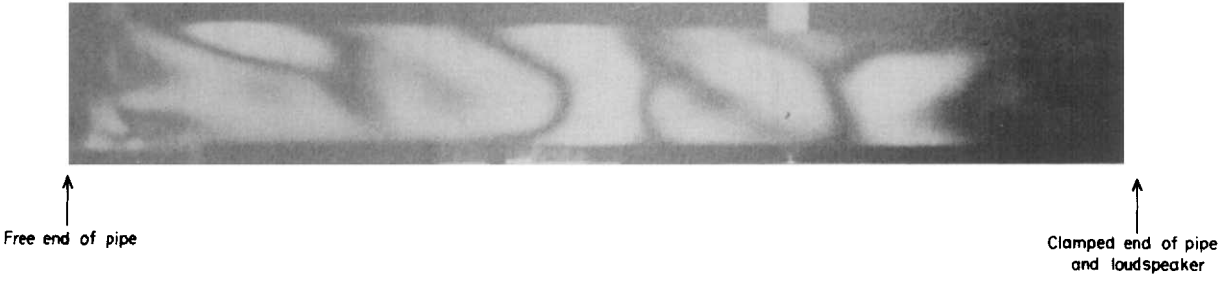

Figure 10. Holographic visualization of acoustically-excited pipe vibration at 3483 Hz.

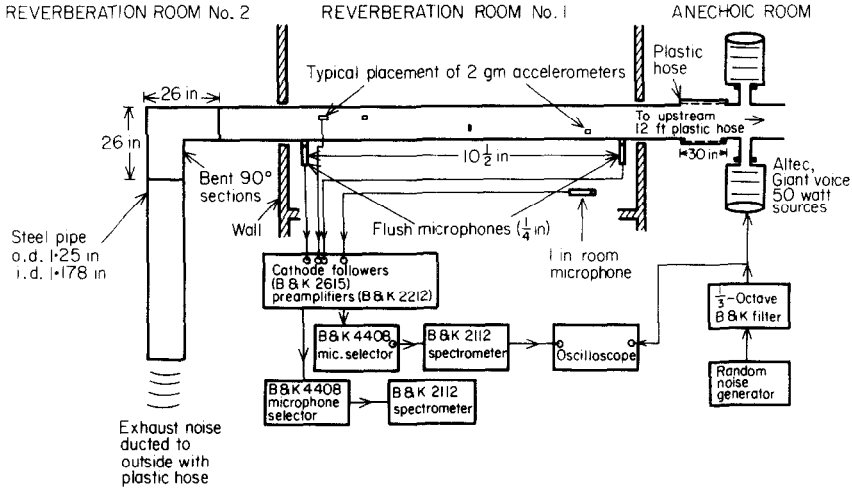

Figure 11. Experimental arrangement for later measurements of sound transmission.

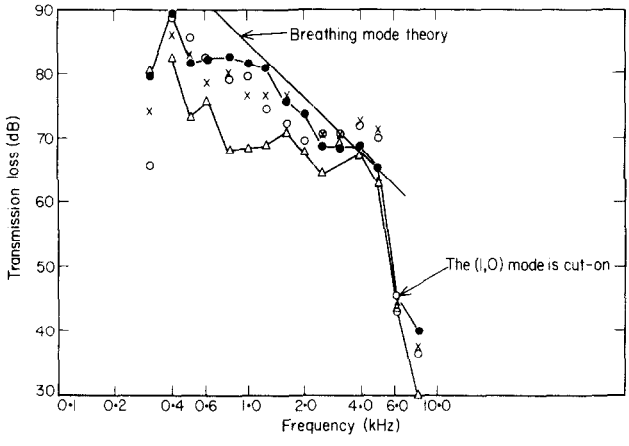

Figure 12. Third-octave transmission loss measurements with and without addition of bend beyond test section. Code: Straight pipe, ●; pipe plus 90° bend, × ($R_B/r_i = 17$); ○ ($R_B/r_i = 4{\cdot}2$); △(mitred bend). Breathing-mode prediction is shown as a solid line, ——.

(1,0) acoustic mode.† Once the mode propagates, it is able to excite pipe bending waves over the whole length of the test section.

Evidence that pipe bending waves are responsible for the additional low-frequency radiation, over and above the breathing mode prediction, is provided by the radiation efficiency measurements shown in Figure 13. The σ measurements up to 2 kHz generally lie close to the σ_1 line predicted for bending motion of the pipe‡, whereas the breathing-mode prediction ($\sigma_0 \doteq \frac{1}{2}\pi k_0 r_0$) is considerably higher over the same frequency range. The data are consistent with the idea that bending waves contribute a significant fraction, say β, of the total sound power radiated, and at the same time dominate the mean square velocity measurement. Given that higher-order pipe response modes ($n \geqslant 2$) make a negligible contribution to $\langle u^2 \rangle$,

† The (1,0) cut-off frequency is 6·7 kHz, which falls in the 6·3 kHz third-octave band.

‡ Based on the small $k_0 r_0$ approximation, $\sigma_1 \doteq \frac{1}{2}\pi(k_0 r_0)^3(1 - f_{cr}/f)$, which gives the radiation efficiency of free bending waves on an infinite thin-walled cylinder above the critical frequency. In the present case $f_{cr} = 325$ Hz (see Appendix II), and at this frequency the ratio of pipe length to wavelength is about 4.

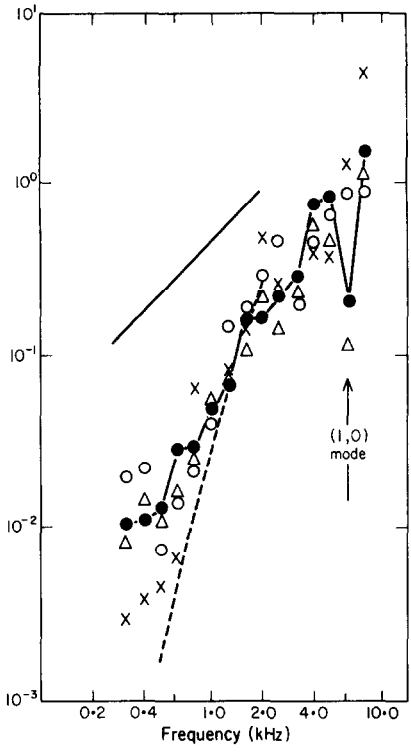

Figure 13. Third-octave radiation efficiency measurements with and without addition of bend beyond test section. Code: As Figure 12. Breathing, bending mode predictions are shown as ——, ---- respectively.

their low radiation efficiency ensures a negligible contribution to W_{rad}, and we may therefore write

$$\sigma \doteq \{\langle u_0^2\rangle \sigma_0 + \langle u_1^2\rangle \sigma_1\}/\langle u_1^2\rangle \doteq \sigma_1/\beta. \tag{5}$$

It follows that if β is not much less than 1—as appears from Figure 12 to be the case up to 2 kHz, even for the straight pipe—a value of σ not much greater than σ_1 is to be expected.

It is worth noting that the $n = 2$ and $n = 3$ pipe response modes have cut-off frequencies of 2·6 kHz and 7·3 kHz, respectively†, and would therefore not be expected to contribute significantly to the measured response, $\langle u^2\rangle$, below these frequencies. The tendency for σ in Figure 13 to drop below σ_1 in the 2·5 kHz band, particularly with the mitred bend attached, may reflect the presence of a significant $\langle u_2^2\rangle$ contribution (compare Figure 10).

3.3.2. *Rigid coupling to source*

The straight pipe and mitred bend TL measurements were repeated with the plastic hose removed, so that the source section was rigidly coupled to the test pipe. Figure 14 summarizes the results.

A simple hypothesis for the combined effects of rigid source coupling and a bend in the pipe is that their effects are additive in terms of sound power radiated from the test section, but Figure 15 shows that this underestimates the radiation, typically by 5 dB. A possible explanation for Figure 15 is that the bending modes of the pipe are less heavily damped in the absence of the plastic hose coupling, so that the mitred bend generates higher vibration levels with the rigid coupling than with the plastic hose.

The same data are presented in an alternative manner in Figure 16. There is remarkable

† See Appendix II.

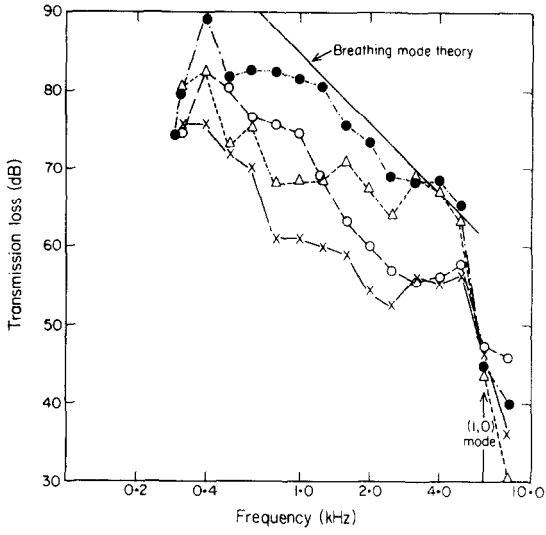

Figure 14. Third-octave transmission loss measurements with and without plastic hose decoupling section between source and test pipe. Code: Straight pipe with source decoupled, ●; source rigidly coupled, ○. Pipe plus 90° mitred bend with source decoupled, △; source rigidly coupled, ×.

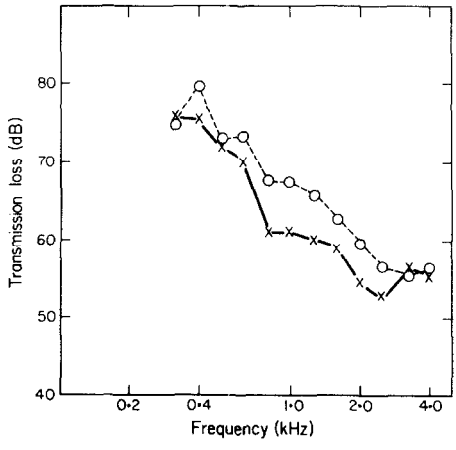

Figure 15. Test of energy addition hypothesis for combined effect of mitred bend and rigid source coupling. Measured TL values for this configuration are shown as —×—. The broken line ---- shows the TL predicted from the equation $w(\times) = w(\triangle) + w(\circ) - 1$, where w is the ratio of W_{rad}/W_{int} at any frequency to the straight-pipe decoupled value (● in Figure 14); $w(\times, \triangle, \circ)$ refer to the configurations in Figure 14.

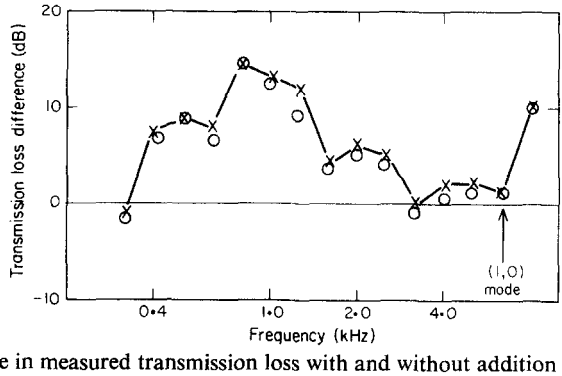

Figure 16. Difference in measured transmission loss with and without addition of 90° mitred bend to test section. Code: Source decoupled, ×; source rigidly coupled, ○.

agreement between the ΔTL values (i.e., straight pipe *minus* pipe with bend) as measured with and without the hose coupling. Whether this is a conicidence is not yet clear, but what Figure 16 does show clearly is that in both configurations, adding a mitred 90° bend to the test pipe increases the sound transmission mainly in the range 400–1250 Hz. Further work is required to establish a theoretical model for bending-wave generation by plane sound waves incident on pipe bends, so that this effect may be explained quantitatively.

4. CONCLUSIONS

(1) Low-frequency airborne sound transmission through cylindrical steel pipe walls is likely under practical conditions to be dominated by bending wave radiation, even though the (1,0) acoustic mode in the pipe is cut off.

(2) By taking extreme care to maintain axial symmetry, and by eliminating bending waves set up by the near field of the sound source, the transmission loss (TL) as defined in equation (2) can be brought close to the breathing-mode limit at low frequencies ($k_o r_i < 1$). Otherwise, the TL may be reduced by as much as 30 dB.

(3) The breathing-mode TL represents an upper limit for low frequencies, which may serve as a standard for judging the acoustic quality of a piping system.

(4) The fact that the breathing-mode TL limit was approached in the present experiments with cold-rolled straight steel pipe suggests that non-uniformities in curvature and wall thickness are of minor significance in piping of this standard, as far as sound transmission is concerned.

(5) Addition of a mitred 90° bend to a straight pipe was found to cause significant increases in 1/3 octave radiated sound power, for the same internal sound pressure level. The effect was most pronounced in the range $k_o r_i = 0{\cdot}1$ to $0{\cdot}4$, where the radiated power exceeded the breathing-mode prediction by up to 20 dB.

(6) Radiused 90° bends ($R_B/r_i = 17, 4{\cdot}2$) generally produced TL values intermediate between the mitred-bend measurements and the breathing-mode prediction.

(7) Further work is required to quantify the generation of pipe bending waves by internally-propagating plane waves of sound incident on a bend.

ACKNOWLEDGMENTS

The authors gratefully acknowledge the financial support of the Science Research Council, U.K. The authors also thank Dr C. R. Hazell and the Royal Aircraft Establishment at Farnborough for their technical support with the holographic measurements.

REFERENCES

1. L. Cremer 1955 *Acustica* **5**, 245–256 (in German). Theory of sound transmission through cylindrical shells.
2. M. Heckl 1958 *Acustica* **8** (Heft 1), 259–265 (in German). Experimental investigation of sound transmission through cylinders.
3. D. J. Small 1971 Personal communication.
4. C. L. Morfey 1971 *Proceedings of the Seventh International Congress on Acoustics, Budapest, Paper* 24 *A* 9. Transmission through duct walls of internally-propagated sound.
5. G. L. Brown and D. C. Rennison 1974 *Proceedings of the Noise, Shock and Vibration Conference, Monash University, Melbourne*, 416–425. Sound radiation from pipes excited by plane acoustic waves.
6. V. I. Gel'fgat, D. R. Guzhas, R. N. Mikhailov and B. D. Tartakovskii 1972 *Soviet Physics—Acoustics* **17**, 464–467. Acoustic reduction of an internally excited closed cylindrical shell.

7. P. W. SMITH, JR. 1957 *Journal of the Acoustical Society of America* **29**, 721–729. Sound transmission through thin cylindrical shells.
8. LORD RAYLEIGH 1877 *Theory of Sound, Volume I.* London: Macmillan.
9. LORD RAYLEIGH 1894 *Theory of Sound, Volume I* (Second edition). London: Macmillan.

APPENDIX I: LIST OF SYMBOLS

a	mean radius of pipe, $\frac{1}{2}(r_i + r_o)$
c_L	value of $(E/\rho)^{1/2}$ for pipe wall material
c_o	sound speed of fluid (same inside pipe as outside, unless otherwise stated)
E	Young's modulus
f	frequency
f_{cr}	bending-wave critical frequency
f_R	ring frequency $c_L/2\pi a$
h	pipe wall thickness
k_o	acoustic wavenumber ω/c_o
k_t	wavenumber on surface of cylinder, $(k_x^2 + n^2/a^2)^{1/2}$
k_x	axial wavenumber
n	circumferential mode order
p	fluctuating pressure
R_B	radius of bend
r_i, r_o	inner, outer radius of pipe
S	pipe cross-sectional area, πr_i^2
S_{rad}	radiating surface area of pipe
TL	transmission loss, equation (2)
U	pipe flow velocity
u	normal velocity of outer surface
W_{int}	total sound power flow in pipe
W_{rad}	sound power radiated from outer surface
Z_τ	transmission impedance, equation (A2)
β	fraction of W_{rad} due to bending waves
γ	wall thickness parameter, equation (A4)
ν	Poisson's ratio
ρ_o	density of fluid
ρ_s	density of pipe wall material
σ	radiation efficiency, equation (3)
ω	radian frequency
Subscripts	
i, o	inside, outside of pipe
n (= 0, 1, 2, ...)	circumferential mode number

APPENDIX II: PIPE STRUCTURAL RESPONSE RELATIONS

TRANSMISSION IMPEDANCE OF CYLINDRICAL SHELL

The elastic response of a thin-walled circular cylinder, infinite in the axial (x) direction, to a differential pressure distribution

$$\Delta p = (p_i - p_o) \propto \exp i(\omega t - k_x x - n\phi), \tag{A1}$$

is characterized by the transmission impedance

$$Z_\tau(n, k_x, \omega) = \Delta p/u. \tag{A2}$$

For any particular n, setting $Z_\tau = 0$ gives a dispersion relation between k_x and ω for free wave motion on the cylinder (neglecting fluid loading).

The thin-walled cylinder approximation implies that the wall thickness h is small compared with both the mean radius a and the wall bending wavelength; thus we assume

$$\gamma^2 \ll 1, \quad |k_x a|^2 \gamma^2 \ll 1, \quad n^2 \gamma^2 \ll 1, \tag{A3}$$

where γ is a wall thickness parameter defined by

$$\gamma = (1 - \nu^2)^{-1/2}(h/12^{1/2}\,a) \tag{A4}$$

($\doteq 0{\cdot}018$ for the thin-walled pipe). For frequencies less than or comparable with the ring frequency ($f_R = c_L/2\pi a$, $\doteq 53{\cdot}5$ kHz for the pipes used in the present tests), relatively simple expressions can be derived for Z_τ. Thus Smith's modification [7]† of Cremer's analysis [1] yields, for non-axisymmetric modes ($n \neq 0$),

$$Z_\tau/\mathrm{i}\omega\rho_s h \doteq 1 + (k_t a)^{-2} - (c_L/\omega a)^2\{(k_x/k_t)^4 + \gamma^2[(k_t a)^4 - 2n^2 + 1]\}, \tag{A5}$$

where $k_t^2 = k_x^2 + (n/a)^2$. Equation (A5) is subject to the low frequency restrictions

$$\omega a/c_L \lesssim 1, \qquad |\omega/c_L k_t|^2 \ll 1. \tag{A6}$$

For axisymmetric cylinder modes ($n = 0$), the wall bending stiffness is unimportant as long as $|k_x a| \lesssim 1$. In this case Cremer's analysis yields directly

$$Z/\mathrm{i}\omega\rho_s h \doteq 1 - (c_L/\omega a)^2[1 - (\omega/c_L k_x)^2]/[1 - (1 - \nu^2)(\omega/c_L k_x)^2], \tag{A7}$$

with no further restrictions beyond the thin-shell limitation mentioned earlier.

AXISYMMETRIC RESPONSE TO PLANE SOUND WAVES PROPAGATING INSIDE CYLINDER

If $\rho_s h \gg \rho_0 a$ (as is the case for all the experiments described), and also $c_L > c_0$ (for steel cylinders in air $c_L/c_0 \doteq 15$), the propagation of plane waves within the cylinder below the ring frequency is not significantly affected by the yielding of the cylinder walls. Thus the axial phase speed ω/k_x of the driving pressure is approximately c_0, and equation (A7) gives as a low-frequency approximation

$$Z_\tau/\mathrm{i}\omega\rho_s h \doteq (\omega a/c_L)^{-2}[1 - (c_0/c_L)^2]/[1 - (1 - \nu^2)(c_0/c_L)^2], \tag{A8}$$

valid for $(\omega a/c_L)^2 = (f/f_R)^2 \ll 1$.

Since $(c_0/c_L)^2$ is small for steel cylinders in air, the second factor on the right of expression (A8) has been approximated by unity in deriving equation (4).

FREE WAVES ON CYLINDER IN THE ABSENCE OF FLUID LOADING

Dispersion relations for free waves on cylinders *in vacuo* are obtained from equations (A5) and (A7) as follows.

$n = 0$.

$$k_x = (\omega/c_L)\{[1 - (1 - \nu^2)(\omega a/c_L)^2]/[1 - (\omega a/c_L)^2]\}^{1/2} \tag{A9}$$

($\doteq \omega/c_L$ for frequencies well below the ring frequency).

$n \neq 0$. We consider only the case of small axial wavenumbers (i.e., $|k_x a|^2 \ll n^2$), in order to illustrate the nature of the dispersion relation near cut-off. Equation (A5) then gives

$$(n^4 + n^2)^{-1}(k_x a)^4 + \gamma^2 F(n)(k_x a)^2 = (\omega^2 - \omega_n^2)(a/c_L)^2; \tag{A10}$$

here

$$\omega_n = (\gamma c_L/a)(n^3 - n)/(n^2 + 1)^{1/2} \tag{A11}$$

defines the cut-off frequency of the nth circumferential bending mode—compare with reference [8], section 233.‡ The funtion $F(n)$, $= 2n^4/(n^2 + 1) + (n^2 - 1)^2/(n^2 + 1)^2$, is positive for all n so that equation (A10) predicts real values of k_x only when $\omega > \omega_n$.

† Smith improved the accuracy of the wall bending term given by Cremer; the difference can be significant for circumferential modes of low order. Note that one of the bending terms is missing from Smith's final expression (16).

‡ The extensional cut-off frequencies $\omega_n' = (c_L/a)\{(1 + n^2)/(1 - \nu^2)\}^{1/2}$, which are also discussed by Rayleigh —see section 235e of reference [9]—are not given by expression (A5) because of the low-frequency restriction $|\omega/c_L k_t|^2 \ll 1$.

$n = 1$. This case is covered by equations (A10) and (A11), but deserves special mention because the cut-off frequency is zero. The $n = 1$ mode corresponds to bending of the cylinder as a beam; the axial wavenumber k_x for free bending waves is given by

$$(k_x a)^2 \simeq 2^{1/2}(\omega a/c_L), \qquad \gamma^2 \ll \omega a/c_L. \tag{A12}$$

Equation (A12) may be used to calculate the bending-mode critical frequency: i.e., the frequency above which the axial phase speed of free bending waves exceeds the speed of sound in the ambient fluid. Hence $f_{cr} \simeq c_o^2/(2^{1/2}\pi c_L a)$, $\doteq 325$ Hz for the pipes used.

EFFECT OF CIRCUMFERENTIAL MODE ORDER ON CYLINDER IMPEDANCE

For a given forcing frequency, ω, and axial wavenumber, k_x, it is of interest to compare the impedances of different non-axisymmetric cylinder modes as given by equation (A5). Provided ω is well below the value at which $Z_\tau(k_x)$ vanishes for all the circumferential modes of interest, the impedance is stiffness controlled; if further the wavenumber is large enough that

$$k_x a > n^2 \gamma^{1/2}, \tag{A13}$$

the stiffness is dominated by wall stretching rather than wall bending, and Z_τ decreases ($\sim n^{-4}$) as n increases.

Since condition (A13) generally holds for a large number of circumferential modes, both for flow noise excitation (where $k_x a \simeq \omega a/U$) and for acoustic excitation by internally propagating duct modes ($k_x a \simeq \omega a/c_i$), it is to be expected in these situations that the low-frequency vibrational response will be spread over a wide range of n values.